

## Spin Physics with the STAR detector

L.C. BLAND<sup>\*)</sup>, for the STAR collaboration

*Department of Physics, Indiana University, Bloomington, IN USA*

The STAR detector will bring unique capabilities to the study of  $\vec{p} + \vec{p}$  collisions up to total center of mass energies of 500 GeV at RHIC. The large acceptance of the time projection chamber and the electromagnetic calorimeter enable STAR to observe jets, and to detect photons and electrons in important regions of phase space. The premier experiments of the STAR spin program are discussed in this contribution. Photon + jet coincidence measurements will provide the world's best determination of the contribution gluons make to the proton's spin. Detection of the daughter electrons and positrons from  $W^\pm$  decay will enable the determination of the polarization of the  $q\bar{q}$  sea within the proton.

### §1. Introduction

With the addition of Siberian Snakes and spin rotators, the Relativistic Heavy Ion Collider (RHIC) at Brookhaven National Laboratory will have the unique capability of accelerating intense polarized proton beams up to energies of 250 GeV per beam. A series of experiments studying  $\vec{p} + \vec{p}$  collisions at energies up to  $\sqrt{s} = 500$  GeV will then be possible at the PHENIX and STAR detectors. The luminosities expected for the RHIC spin program (up to  $2 \times 10^{32} \text{cm}^{-2} \text{s}^{-1}$  at  $\sqrt{s} = 500$  GeV) will enable the study of *polarization observables* for large transverse momentum ( $p_T$ ) processes, where perturbative QCD methods have been successfully applied to explain most *unpolarized* observables in  $p + \bar{p}$  collisions. One of the polarization observables that will be measured at RHIC is the parity-allowed longitudinal spin correlation

$$A_{LL} = \frac{1}{P^2} \frac{N_{++} - N_{+-}}{N_{++} + N_{+-}}, \quad (1)$$

where  $P$  represents the beam polarizations assumed to be the same for both longitudinally polarized beams in Eqn. 1. The RHIC-spin project will theoretically provide  $P = 0.70$  for each beam. The spin correlation coefficient,  $A_{LL}$ , requires measuring the difference in yield for some process for equal ( $N_{++}$ ) and opposite ( $N_{+-}$ ) proton beam helicities. Parity-violating single-spin longitudinal asymmetries ( $A_L$ ) have a similar form to Eqn. 1, but require that only one beam be polarized.

This contribution discusses the capabilities the STAR detector brings to the RHIC-spin program. When the construction of the barrel and endcap electromagnetic calorimeters are completed, STAR will have unique capabilities for the study of large- $p_T$  processes in  $\vec{p} + \vec{p}$  collisions. In addition to critical tests of QCD, the STAR detector will study processes that will enable the untangling of the spin structure of the proton. In particular, the study of the  $\vec{p} + \vec{p} \rightarrow \gamma + \text{jet} + X$  reaction at  $\sqrt{s} = 200$  and 500 GeV will provide the world's best determination of the fraction of the proton's

---

<sup>\*)</sup> E-mail address: bland@iucf.indiana.edu

spin carried by gluons. Measurement of polarization observables for inclusive jet and di-jet production will provide important cross checks on the gluon polarization. In addition, the study of parity violating spin asymmetries in  $W^\pm$  production will help unravel the spin-flavor content of the  $q\bar{q}$  sea within the proton. These spin structure function studies are the next essential step in understanding the internal structure of the proton.

The present understanding of the proton's spin structure comes from years of polarized deep-inelastic scattering (pDIS) experiments at CERN, SLAC and more recently the HERMES experiment at HERA<sup>1)</sup>. A global analysis of the inclusive pDIS data suggests that the quarks account for only a small fraction of the proton's spin, assuming that the gluon polarization is zero. This deficiency can be rectified if the gluon polarization is large, and there are canceling contributions to the proton spin arising from orbital angular momentum. The crucial next step in understanding the proton's spin structure is to measure the gluon polarization. The goal is the determination of the *integral*  $\Delta G$ , defined as

$$\Delta G(Q^2) = \int_0^1 \Delta G(x, Q^2) dx = \int_0^1 [G^+(x, Q^2) - G^-(x, Q^2)] dx, \quad (2)$$

related to the total contribution gluons make to the proton's spin, at the scale  $Q^2$ . (Hereafter, the  $Q^2$  dependence of these quantities will be suppressed for clarity.) The fraction of the proton's longitudinal momentum carried by the gluon is  $x$ . In Eqn. 2, the gluon helicity asymmetry distribution ( $\Delta G(x)$ ) is given by the difference in probability of finding a gluon with its polarization parallel ( $G^+$ ) versus antiparallel ( $G^-$ ) to the proton's longitudinal polarization. The unpolarized gluon probability distribution is defined as  $G(x) = G^+(x) + G^-(x)$ . The gluon polarization at a given  $x_{gluon}$  is  $\Delta G(x)/G(x)$ .

Several ideas exist for probing the gluon polarization. Although gluons are not electrically charged, they can be directly probed in polarized lepton scattering experiments using the so-called photon-gluon fusion (PGF) process. The COMPASS experiment<sup>2)</sup> will attempt to study this process by detecting the leading hadrons from the  $q$  and  $\bar{q}$  jets produced in PGF. The range of  $x_{gluon}$  covered by COMPASS will prevent a determination of the integral in Eqn. 2. COMPASS will have sensitivity to the gluon polarization at relatively large  $x_{gluon}$ , and hence will be insensitive to the  $x$  range where the gluons become increasingly abundant. Even though the gluon polarization is small at small  $x$ , there are critical contributions to the integral in Eqn. 2, as  $x \rightarrow 0$ . The best determination of the integral  $\Delta G$  requires sensitivity to the gluon polarization over a broad range of  $x_{gluon}$ .

An alternate method for determining  $\Delta G(x)$  is to study pDIS over a very broad range of  $x_{quark}$  and  $Q^2$ . The gluon helicity asymmetry distribution could then be extracted by an analysis of the scaling violations in pDIS. Existing measurements of pDIS do not span a broad enough range of  $Q^2$  to provide an accurate determination of  $\Delta G(x)$ . The necessary pDIS measurements could be made at HERA in the study of  $\vec{e} + \vec{p}$  collisions, if the 820 GeV proton beam were polarized. A decision to take this challenging step will not be made until 2002.

In the absence of a 'polarized HERA collider', the best determination of the

integral  $\Delta G$  will come from the study of photon production in  $\vec{p} + \vec{p}$  collisions at RHIC, as described below.

## §2. The STAR detector

STAR is one of the two large detectors at RHIC designed for relativistic heavy-ion collisions to isolate and study the quark-gluon plasma. As is also true for PHENIX, the capabilities of the STAR detector will allow its use for the study of many of the interesting processes in  $\vec{p} + \vec{p}$  collisions. The large acceptance of the STAR detector makes it suitable for reconstructing the hadronic jets that are prolifically produced in high- $p_T$  processes. The STAR electromagnetic calorimeter will be used to detect high- $p_T$  photons and the  $e^\pm$  daughters of the  $W^\pm$  bosons produced in  $\vec{p} + \vec{p}$  collisions. In addition, the  $e^+e^-$  pairs produced in either the Drell-Yan or real  $Z^0$  production can be detected with the large acceptance of the STAR EMC.

The heart of the STAR detector is the world's largest time projection chamber. The TPC provides tracking through a 0.5 T solenoidal magnetic field of the thousands of charged particles that are produced in a single Au-Au collision. The TPC will play an important role in the STAR-spin program, tracking the charged hadrons produced by jets over the pseudorapidity interval  $-1.8 \lesssim \eta \lesssim 1.8$ . Photons and electrons will be detected by the STAR electromagnetic calorimeter (EMC). The barrel EMC construction is well underway, and will ultimately result in 120 modules spanning  $2\pi$  in azimuth and the pseudorapidity interval,  $-1 \leq \eta \leq +1$ . At present, a patch of the BEMC consisting of four modules is installed in the STAR detector. The patch covers  $0 \leq \eta \leq +1$ , with an azimuthal extent of 0.42 radians. The BEMC patch will be in operation for the first Au-Au collisions in the year 2000.

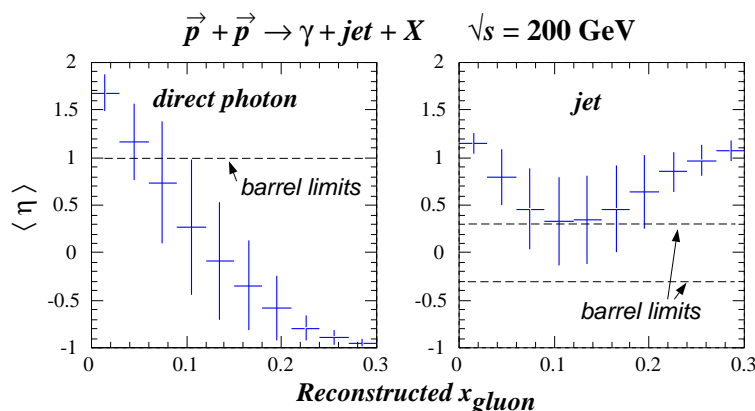


Fig. 1. Moments of the pseudorapidity distribution of simulated photon-jet coincidence events contributing to each bin in reconstructed  $x_{gluon}$  values. Each point represents the mean contributing  $\eta$  value for photons or jets, with the 'error' bars reflecting the rms deviation from the mean.

Recently, funding for the STAR endcap EMC was approved. When its construction is complete, the EEMC will span the pseudorapidity interval,  $1.07 \leq \eta \leq 2$ , covering the full azimuth, and will provide access to *asymmetric partonic collisions*

for ‘direct photon’ and  $W^\pm$  production processes. The EEMC provides critical phase space coverage for both  $\gamma$ +jet and  $W^\pm$  production studies. By detecting large- $p_T$  processes at forward angles, asymmetric initial states, where one parton has a larger  $x$  than the other, are emphasized. For photon production, such collisions effectively select large- $x$  quarks as an *analyzer* of the polarization of small- $x$  gluons. In addition to kinematic selection of quarks with large polarization (the pDIS asymmetry  $A_1^p$  increases with increasing  $x_{quark}$ ), the EEMC will detect photons produced at partonic CM angles where the partonic-level spin correlation parameter ( $\hat{a}_{LL}$ ) approaches its maximum value, unlike the situation encountered for midrapidity photon production.

The large acceptance of STAR is critical for the measurement of the away-side jet in coincidence with the produced photon (Fig. 1). Coincident  $\gamma$ +jet detection allows for the reconstruction of the initial-state partonic kinematics. With the momentum fractions  $x_{quark}$  and  $x_{gluon}$  determined by the experiment, a more direct connection between the measured polarization observables and the gluon helicity asymmetry distribution can be made. This is advantageous to in trying understand how the measurement errors will influence the determination of  $\Delta G(x)$ .

### §3. Gluon polarization measurements at STAR

The existing data for scaling violations in pDIS provide only very loose constraints on  $\Delta G(x)$ . Several analyses of these constraints have been made <sup>3),4)</sup> and have generally concluded that the *integral*  $\Delta G$  is positive. The variation of the gluon helicity asymmetry distribution with the gluon momentum fraction ( $x_{gluon}$ ) has significant differences in these different analyses. There is generally always a positive peak of  $x\Delta G(x)$ , but the  $x_{gluon}$  value of the peak is not well constrained. Consequently, the gluon *polarization*,  $(\Delta G(x)/G(x))$  can be either large or small, depending on where the peak in  $x\Delta G(x)$  occurs. Many parameterizations of  $\Delta G(x)$  that are consistent with existing measurements result in negatively polarized gluons at some  $x_{gluon}$  values. In leading order perturbative QCD (pQCD), the spin correlation parameter ( $A_{LL}$ ) that will be measured in  $\vec{p} + \vec{p} \rightarrow \gamma + X, \gamma + \text{jet} + X$  reactions at RHIC is proportional to the gluon polarization.

To illustrate the sensitivity of  $\gamma$  + jet coincidence measurements planned for STAR, simulations using the three  $\Delta G(x)$  models in Ref. <sup>4)</sup> (hereafter referred to as GS sets A,B and C) have been performed. In all cases, the input  $\Delta G(x)$  must be

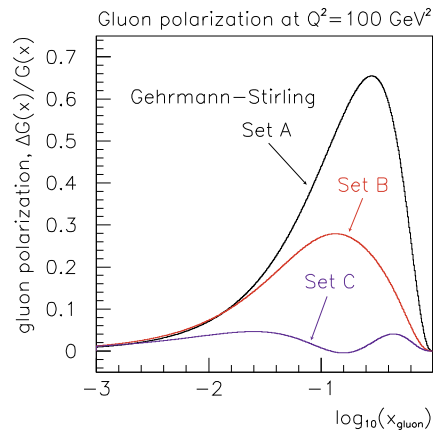


Fig. 2. Gluon polarizations computed from models of  $\Delta G(x)$  consistent with polarized deep inelastic scaling violations<sup>4)</sup>. The structure functions are evolved to the scale that will be probed at RHIC.

evolved<sup>5)</sup> from the scale where the analysis was performed,  $Q_0^2=4 \text{ GeV}^2$ , to the scales that will be probed at RHIC, taken to be  $Q^2=p_{T,\gamma}^2/2$ , where  $p_{T,\gamma}$  is the transverse momentum of the photon. The variation of the resulting gluon polarization with  $x_{gluon}$  for the three  $\Delta G(x)$  models in Ref. <sup>4)</sup>, evolved to  $Q^2=100 \text{ GeV}^2$ , is shown in Fig. 2.

The simulated spin correlation coefficient<sup>6)</sup> expected for inclusive photon production in  $\vec{p} + \vec{p}$  collisions at RHIC, using the GS-A,B and C models of  $\Delta G(x)$ , is shown in Fig. 3 as a function of  $x_T = 2p_{T,\gamma}/\sqrt{s}$ . The variable  $x_T$  is often interpreted as the initial-state parton momentum fraction. This applies only for midrapidity photons, and is only true when averaging over an event ensemble. The simulations include the subprocesses  $fg \rightarrow f\gamma$  (where  $f$  refers to either a quark or an antiquark),  $q\bar{q} \rightarrow g\gamma$  and  $q\bar{q} \rightarrow \gamma\gamma$ , hereafter referred to as ‘direct photon’ processes. The first of these subprocesses provides  $\sim 90\%$  of the direct photon yield. The magnitude of the calculated  $A_{LL}$  in the pseudorapidity range covered by the STAR EEMC is larger than at midrapidity, as expected since the endcap selects events having more asymmetric  $qg$  collisions and having partonic scattering angles where  $\hat{a}_{LL}$  (the pQCD result for the partonic spin correlation coefficient) is large. The predicted decrease in  $A_{LL}$  as one goes from GS set A, to set B and then set C for  $\Delta G(x)$ , simply reflects the smaller gluon *polarization vs  $x_{gluon}$*  in those three models (Fig. 2).

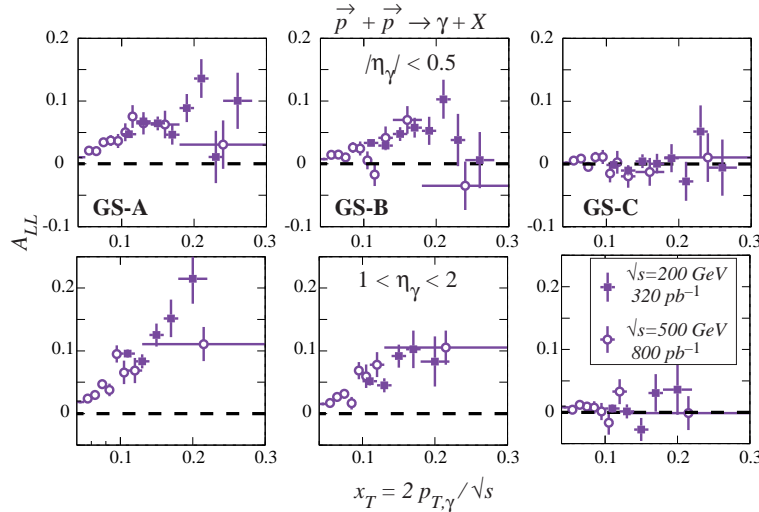


Fig. 3. Simulated values for  $A_{LL}$  for inclusive photon production at RHIC energies. The top row shows the spin correlations for midrapidity photons that can be detected at both PHENIX and STAR. The bottom row shows expected values at the forward angles probed by the STAR EEMC. Not evident in this figure, is that for a given  $x_T$ , photons detected in the EEMC correspond to smaller- $x$  gluons than those detected at midrapidity.

As discussed elsewhere<sup>6), 7)</sup>, STAR will be able to detect a significant fraction of the away-side jets in coincidence with the produced photon. This capability results from the large phase space coverage of the existing time-projection chamber and the planned electromagnetic calorimetry. Detection of  $\gamma$ +jet coincidences enables the reconstruction of the initial-state partonic kinematics<sup>6)</sup>. With this capability, a direct

extraction of  $\Delta G(x)$  can be made from the measured  $A_{LL}$ , assuming contributions from only quark-gluon Compton scattering and collinear initial-state parton collisions. Excluding experimental backgrounds, there remain small contributions to the  $\gamma$ +jet yield from partonic subprocesses other than quark-gluon Compton scattering. The  $q\bar{q}$  annihilation contribution can be corrected for based on simulations. Fig. 4 shows the directly extracted  $\Delta G(x)$  from the simulated  $A_{LL}$  values, after applying an additive correction for  $q\bar{q}$  annihilation. A  $320 \text{ pb}^{-1}$  sample at  $\sqrt{s} = 200 \text{ GeV}$  and a  $800 \text{ pb}^{-1}$  sample at  $\sqrt{s} = 500 \text{ GeV}$  have been combined in the figure. These data samples can be achieved in two ten week runs, based on the projected luminosity for  $\vec{p} + \vec{p}$  collisions. The latter is especially crucial to extend the coverage to small  $x_{gluon}$  values.

To ascertain the sensitivity STAR will have to the fraction of the proton's spin carried by gluons (or, the *integral*  $\Delta G$ ), the results in Fig. 4 were fitted to a standard structure function parameterization<sup>4)</sup>,

$$x\Delta G(x) = \eta A x^a (1-x)^b [1 + \rho x^{1/2} + \gamma x],$$

$$\text{with } A^{-1} = \left(1 + \frac{\gamma a}{a+b+1}\right) \frac{\Gamma(a)\Gamma(b+1)}{\Gamma(a+b+1)} + \rho \frac{\Gamma(a+\frac{1}{2})\Gamma(b+1)}{\Gamma(a+b+1)}. \quad (3)$$

The resulting fitted value for  $\eta$  represents the integral  $\Delta G$ . In Eqn. 3, the  $b$  and  $\gamma$  parameters are held fixed at values obtained by evolving<sup>5)</sup> the  $\Delta G(x)$  input to the simulation to the  $Q^2$  values relevant at RHIC. The  $b$  parameter specifies the large- $x$  behavior of  $\Delta G(x)$ . The fixed parameters used in the fits are consistent with positivity constraints ( $|\Delta G(x)| < G(x)$ ).

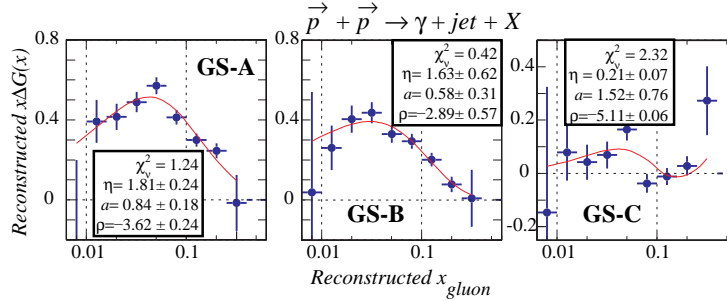


Fig. 4. Fits to the reconstructed  $\Delta G(x)$  directly reconstructed from the simulated  $A_{LL}$  for  $\gamma$ +jet coincidences, after correcting for  $q\bar{q}$  annihilation. A standard parameterization is used to fit the data, with the parameters specifying the large  $x_{gluon}$  behavior fixed. Full data sets for  $\sqrt{s}=200$  (500) GeV are assumed, corresponding to integrated luminosity of  $320$  ( $800$ )  $\text{pb}^{-1}$

Beyond illustrating the sensitivity of STAR to the fraction of the proton's spin carried by gluons, the analysis presented in Fig. 4 illustrates several other things.

- an accurate determination of  $\Delta G$  will require both  $\sqrt{s}=200$  and  $500 \text{ GeV}$  data samples to get to sufficiently small  $x_g$ . Due to strong correlations between  $\eta$  and  $a$  (specifying the small  $x$  behavior of  $\Delta G(x)$ ),  $\delta\eta$  grows rapidly as the low- $x$  points are successively eliminated. It is critical to observe the falloff of  $x\Delta G(x)$  with decreasing  $x$  to ensure an accurate determination of  $\eta$ .

- *the large- $x$  behavior of  $\Delta G(x)$  must be constrained to determine the integral  $\Delta G$  at RHIC.* The fixed parameters in the above analysis presuppose that the large  $x$  behavior of  $\Delta G(x)$  is known. The COMPASS experiment at CERN<sup>2)</sup> should provide the necessary measurements. Detection of  $\gamma$ +jet coincidences, with the photons observed at negative pseudorapidity (Fig. 1), will provide critical overlap between the STAR and COMPASS results to check the consistency of  $\Delta G(x)$  between the two experiments.
- *Additional corrections must be made to  $\Delta G_{recon}(x)$  to ensure an accurate determination of the integral  $\Delta G$ .* The present analysis neglects several other corrections, including evolving all of the  $\Delta G_{recon}(x)$  points to a common  $Q^2$  and correcting for the kinematic reconstruction errors, because they require knowledge of  $\Delta G(x)$  and hence will require an iterative approach to deduce the result. Even when making these corrections, the fitted  $\eta$ , although closer to the input value, is too small. The largest remaining error comes from neglecting the transverse momentum ( $k_T$ ) of the partons in the initial state. Repeating the analysis with simulations that don't include initial-state parton showers (and hence do not include  $k_T$  smearing) results in a fitted  $\eta$  in agreement with the input  $\Delta G$ .

The end result is, that after accounting for the most significant sources of systematic error<sup>7)</sup>, we expect that the fraction of the proton's spin carried by gluons can be determined to an accuracy of approximately 0.5, primarily based on the STAR measurements of  $\vec{p} + \vec{p} \rightarrow \gamma + \text{jet} + X$ . Data samples at both  $\sqrt{s}=200$  and 500 GeV are crucial so that the accuracy is not limited by extrapolation errors. The analysis of  $\Delta G_{recon}(x)$  presented here is intended to illustrate the sensitivity of the STAR measurements to the integral  $\Delta G$ . Clearly, the best determination of  $\Delta G$  will result from a global analysis of all relevant data.

To achieve this accuracy in the integral  $\Delta G$ , the relatively small  $\gamma$ +jet signal must be extracted from a sizeable background of  $\pi^0(\eta)$ +jet coincidences, where a high- $p_T$  meson can mimic the photon signal by decaying into two closely-spaced photons. Both isolation cuts and observation of the characteristic response of a shower-maximum detector to the showers from the closely spaced photons will be used<sup>6),7)</sup> to discriminate signal from background at STAR. In addition to these experimental backgrounds, other processes will contaminate the quark-gluon Compton scattering signal.

As predicted by several studies<sup>8)</sup>, photons produced in the fragmentation of final state recoiling partons present an important contribution to the total yield, in addition to 'direct photon' processes. The impact of these so-called 'fragmentation photons' on the determination of  $\Delta G(x)$  using  $\gamma$ +jet coincidences at STAR has been ascertained using PYTHIA<sup>9)</sup>. Reliable results are expected from the simulated 'fragmentation photon' yield, since the  $p + \bar{p} \rightarrow \gamma + 2 \text{ jet} + X$  yield measured by CDF<sup>10)</sup> is well represented by PYTHIA.

The 'fragmentation photon' yield is obtained by considering all  $2 \rightarrow 2$  subprocesses, responsible for the bulk of the non-diffractive inelastic cross section, and searching for those events that have an energetic photon that is not produced by the decay of any parent hadron. The detector resolutions and acceptances of STAR are

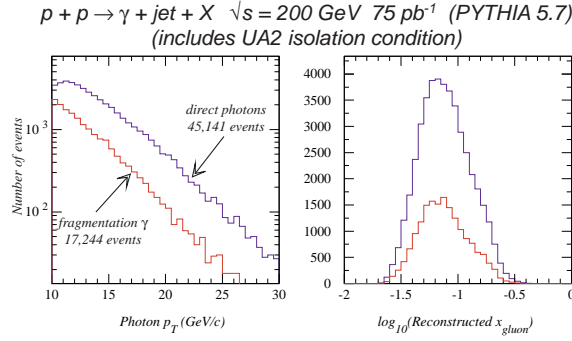


Fig. 5. Comparison between the ‘direct’ and ‘fragmentation’  $\gamma + \text{jet}$  yield that is expected to be observed with the STAR detector. Direct photons are those produced in hard scattering events, predominantly quark-gluon Compton scattering. Fragmentation photons are produced in the fragmentation of recoiling final state partons. It is possible that a more restrictive isolation condition will reduce the contribution from fragmentation photons.

imposed on all observable particles in the event. The away-side jet is reconstructed using the UA1 jet finder, suitably modified for STAR<sup>11)</sup>, and the UA2<sup>12)</sup> isolation condition is imposed on the high- $p_T$  photon candidate. Naively, the latter is expected to effectively eliminate ‘fragmentation photons’, because of the additional hadrons expected within a cone around the photon. Unfortunately, the hardest fragmentation photons result from bremsstrahlung, and are widely displaced from the core of the jet produced by the radiating parton. The end result is that a significant fraction of the overall  $\gamma + \text{jet}$  yield will arise from ‘fragmentation photons’. The comparison between this yield and the ‘direct photon yield’ (defined in the previous section) is shown in Fig. 5. It is possible that an improved isolation condition, beyond the one employed by UA2, can reduce the ‘fragmentation photon’ yield beyond that shown in the figure.

What impact does this background process have on the planned measurement of  $\Delta G(x)$ ? This question was addressed by calculating  $A_{LL}$  for  $\vec{p} + \vec{p}$  collisions including both ‘direct’ and ‘fragmentation’ photon processes. The result for  $A_{LL}$  is shown in Fig. 6, comparing ‘direct photon’ production alone to a calculation combining direct and fragmentation photons. The input  $\Delta G(x)$  corresponds to GS set A<sup>4)</sup>. A small dilution of  $A_{LL}$  is observed from fragmentation photons. Either improved isolation cuts or a more sophisticated analysis of the event topology is expected to reduce the dilution of the direct photon  $A_{LL}$ . The relative importance of the dilution will increase as the gluon polarization decreases.

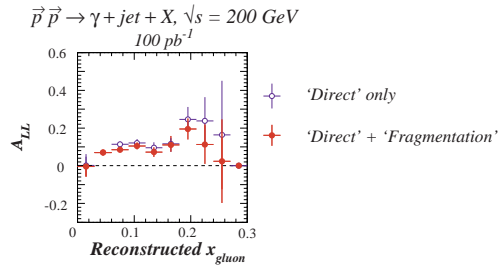


Fig. 6. Calculated  $A_{LL}$  for  $\vec{p} + \vec{p}$  collisions at  $\sqrt{s} = 200 \text{ GeV}$  for ‘direct photons’ only versus ‘direct + fragmentation’ photon production. The sizeable yield of ‘fragmentation photons’ produces a small dilution of  $A_{LL}$ .



#### §4. Partonic kinematics reconstruction in $W^\pm$ production

The Standard Model predicts that  $W^\pm$  bosons are predominantly produced in  $p + p$  collisions by the partonic processes  $u + \bar{d} \rightarrow W^+$  and  $d + \bar{u} \rightarrow W^-$ . Given the  $V - A$  theory of the weak interaction, sizeable *parity violating* longitudinal spin asymmetries,  $A_L$ , are expected in  $\vec{p} + p$  collisions<sup>13)</sup>. These asymmetries can be related to the polarized and unpolarized parton distribution functions, and in certain kinematic domains are directly proportional to either quark or antiquark polarizations<sup>7)</sup> (*ie.*, the ratio of the structure functions  $\Delta f(x)/f(x)$ , where  $f$  represents either  $q$  or  $\bar{q}$ ). Since the partonic constituents of the proton are assumed to have negligibly small transverse momenta, the produced  $W^\pm$  bosons should be collinear with the colliding protons. Higher-order gluon radiation<sup>14)</sup> results in non-zero, but small, values for the  $W^\pm$  transverse momentum, defined as  $q_T$ .

To achieve the goal of determining the unpolarized and polarized parton distribution functions of the nucleon, the variation of these probabilities with Bjorken  $x$ , interpreted as the fraction of the nucleon's longitudinal momentum carried by the parton, and the scale,  $Q^2$  is required. In some cases, this  $x$  dependence is deduced from a theoretical interpretation of experimental observables. The impact of the measurement errors on the deduced structure functions can be best ascertained if these critical kinematic variables can be *directly deduced* from the experiment. For the case of determining the gluon polarization within the proton,  $\gamma$ +jet coincidences provides the necessary kinematic determination. Below, a method is proposed to extract the  $x$  dependence of the polarization of sea antiquarks in the proton. The method relies on measuring only the four momentum of the daughter charged lepton produced in the decay of  $W^\pm$ , and simplifying assumptions about the kinematics.

If the  $W^\pm$  transverse momentum is zero, then by simply measuring the angle and energy of the daughter charged lepton, the longitudinal momentum of the parent  $W^\pm$  can be determined. This, combined with the assumption that the total energy in the partonic CM equals the nominal mass of the  $W$ , allows the Bjorken  $x$  values for the interacting  $q$  and  $\bar{q}$  to be directly deduced. In a real experiment,  $q_T$  can be ignored if it is small compared to the  $W^\pm$  longitudinal momentum,  $p_{L,W}$ . Conveniently, the region of phase space where  $A_L$  can be most directly related to the quark and antiquark polarization corresponds to asymmetric  $q + \bar{q}$  collisions, resulting in large  $p_{L,W}$ . When  $p_{L,W}$  is large,  $q_T$  can be assumed to be zero. The accuracy of this initial-state partonic kinematics reconstruction is shown in Fig. 7. In that figure, an initial-state kinematics reconstruction is applied to  $p + p \rightarrow W^\pm$  events generated by PYTHIA<sup>9)</sup> at  $\sqrt{s}=500$  GeV. The parton shower model is used to simulate higher-order QCD effects responsible for non-zero  $q_T$  values for the  $W^\pm$ . Event selection requires that an  $e^+$  or  $e^-$  be within the acceptance of the STAR barrel and endcap EMC and have  $p_{T,e} \geq 10$  GeV/c. The resolution of the STAR EMC is taken to be  $\delta E_e/E_e = 0.02 + 0.16/\sqrt{E_e}$ . The finite accuracy in the partonic kinematics reconstruction dominantly results from the simplifying assumptions used in the analysis but also has some contributions from the EMC resolution, imposing a performance requirement on the detector.

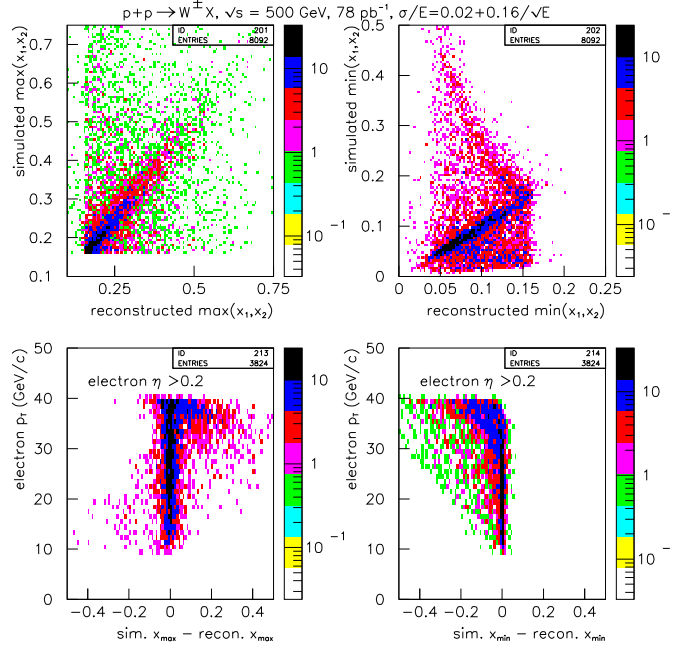


Fig. 7. (Top) Simulated versus reconstructed Bjorken  $x$  values for the  $q$  and  $\bar{q}$  that form the  $W^\pm$  in  $p+p$  collisions. The reconstruction ignores the transverse momentum of the  $W$  ( $q_T$ ). (Bottom) The difference between simulated and reconstructed  $x$  value versus the transverse momentum of the daughter  $e^\pm$  produced by  $W^\pm$  decay. The  $e^\pm$  are detected at  $\eta > 0.2$  to minimize the number of events where the  $W^\pm$  has small longitudinal momentum ( $p_{L,W}$ ). The initial-state kinematics reconstruction fails at midrapidity because  $q_T$  is not small relative to  $p_{L,W}$ .

The critical assumption that  $q_T$  is small works best when the daughter  $e^\pm$  from  $W^\pm$  decay is detected away from midrapidity ( $|\eta| \approx 0$ ). The reason for this is that most of the  $e^\pm$  at large  $\eta$  are produced from  $W^\pm$  created in asymmetric  $q + \bar{q}$  collisions<sup>7)</sup>. These asymmetric collisions provide a sizeable longitudinal momentum to the  $W$ ,  $p_{L,W} = \beta_{pCM} \gamma_{pCM} M_W c$ , where the partonic center of momentum (pCM) is moving with velocity equal to  $\beta_{pCM} c$  and  $\beta_{pCM} = (x_1 - x_2)/(x_1 + x_2)$  in the collider reference frame. The momentum fractions of the  $q$  and  $\bar{q}$  are denoted as  $x_1$  and  $x_2$ . When the daughter  $e^\pm$  are detected near  $|\eta| \approx 0$ , the reconstruction procedure fails because  $p_{L,W}$  is generally small, and  $q_T$  can no longer be ignored. The influence of  $q_T$  on the kinematics reconstruction can be minimized by imposing restrictions on both  $\eta_e$  and  $p_{T,e}$ . The correlation of  $\delta x_{max(min)}$  with  $p_{T,e}$ , for events with  $\eta_e > 0.2$ , is shown in Fig. 7. The kinematics reconstruction is observed to fail at the largest values of  $p_{T,e}$ . The extreme values of the  $e^\pm$  transverse momentum are known to be most sensitive to  $q_T$ <sup>15)</sup>.

Overall, this kinematics reconstruction procedure accurately determines the momentum fractions of the quark and antiquark that form the  $W^\pm$  for most of the events. However, even with restrictions on the pseudorapidity and transverse mo-

mentum of the  $e^\pm$ , events with large  $|\delta x_{\max(\min)}| = |x_{\max(\min)}^{\text{sim}} - x_{\max(\min)}^{\text{recon}}|$  still arise. The reasons for this are: (1) events with sizeable  $q_T$  are predicted to occur by PYTHIA even when the daughter  $e^\pm$  is detected at  $\eta > 0$ , (2) the mass distribution of the  $W$  can result in events with  $M_W$  significantly different from its central value of 80.4 GeV/c<sup>2</sup>, and (3) some of the daughter  $e^\pm$  can be produced by the decay chain  $W^\pm \rightarrow \tau^\pm + \nu_\tau \rightarrow e^\pm + \nu_e + \nu_\tau$  meaning that the  $W$  rest energy is shared between three, rather than two, final state particles. Some additional ambiguity will arise in the assignment of  $x_{\max(\min)}$  to the interacting  $q$  and  $\bar{q}$ . However, for most of the events  $x_{\max}$  will correspond to  $x_q$  and  $x_{\min}$  to  $x_{\bar{q}}$ . To quantitatively assess the efficacy of this kinematics reconstruction procedure, simulations of  $A_L$  using specific models for quark and antiquark structure functions must be performed. The kinematics reconstruction can be used to attempt to directly extract the quark polarization from the simulated  $A_L$  in the appropriate part of phase space.

## §5. Summary

An exciting program of studies in ‘spin physics’ will commence at RHIC in 2001, when the first  $\vec{p} + \vec{p}$  collisions at high energy will be observed by the PHENIX and STAR detectors. The development of the polarization and intensity of the colliding proton beams will parallel the construction of the STAR barrel and endcap electromagnetic calorimeters, and the implementation of other necessary changes to STAR required for the measurement of polarization observables in high-luminosity  $\vec{p} + \vec{p}$  collisions. The present plan is that the RHIC spin program will be more fully developed by 2003. Measurements in the ensuing years will provide important tests of QCD and data that should help to unravel the spin structure of the proton. Possibly the most significant result that will come from the RHIC-spin program is the determination of the fraction of the proton’s spin carried by gluons.

## References

- 1) For a recent review of polarized deep inelastic scattering experiments, see G.G. Petratos, in EPIC99 Proceedings, eds. L.C. Bland, T. Londergan and A. Szczepaniak (World Scientific, Singapore, 2000), and references therein.
- 2) A. Bravar, D. von Harrach and A. Kotzinian, Phys. Lett. **B421** (1998), 349.
- 3) R.D. Ball, S. Forte and G. Ridolphi, Phys. Lett. **B378** (1996), 255.
- 4) T. Gehrmann and W.J. Stirling, Phys. Rev. **D53** (1996), 6100.
- 5) M. Hirai, S. Kumano and M. Miyama, *Comp. Phys. Commun.* **108** (1998), 38.
- 6) L.C. Bland, in EPIC99 Proceedings, eds. L.C. Bland, T. Londergan and A. Szczepaniak (World Scientific, Singapore, 2000). Also available at hep-ex/9907058.
- 7) L.C. Bland, W.W. Jacobs, J. Sowinski, E.J. Stephenson, S.E. Vigdor and S.W. Wissink, *An Endcap Electromagnetic Calorimeter for STAR: Conceptual Design Report*, STAR Note 401 (1999).
- 8) L.E. Gordon and W. Vogelsang, Phys. Rev. **D48** (1993), 3136.
- 9) T. Sjöstrand, *Comp. Phys. Commun.* **82** (1994), 74.
- 10) F. Abe *et al.*, Phys. Rev. **D57** (1998), 67.
- 11) W.B. Christie and K. Shestermanov, STAR Note 196 (1995).
- 12) J. Alitti *et al.*, Phys. Lett. **B299** (1993), 174.
- 13) C. Bourrely and J. Soffer, Phys. Lett. **B314** (1993), 132.
- 14) G. Altarelli, R.K. Ellis and G. Martinelli, Phys. Lett. **B151** (1985), 457.
- 15) B. Abbott *et al.*, Phys. Rev. **D58** (1998), 092003.